PROCEEDINGS, 48th Workshop on Geothermal Reservoir Engineering
Stanford University, Stanford, California, February 6-8, 2023
SGP-TR-224

Distributed Acoustic Sensing Strain Signatures as an Indicator of Fracture Connectivity in Enhanced Geothermal Systems

Megan Ward-Baranyay[1], Matthew Becker[1], Ahmad Ghassemi[2], Jonathan Ajo-Franklin[3], and the FOGMORE team

[1]Department of Geological Sciences, California State University, Long Beach, Long Beach, CA 90840

[2]Reservoir Geomechanics and Seismicity Research Group, The University of Oklahoma, Norman, OK 73069

[3]Department of Earth, Environmental, and Planetary Sciences, Rice University, Houston, TX 77005

matt.becker@csulb.edu

Keywords: DAS, Geothermal, FORGE, EGS, stimulation, modeling and simulation

ABSTRACT

Stimulated fracture connectivity between injector and producer is a critical prerequisite for efficient EGS thermal recovery. Some stimulated fractures may be incomplete, approaching but not intersecting the production well. These "near-miss" fractures can be addressed in future stimulation stages or re-stimulated to complete the connection. We propose the use of fiber optic distributed acoustic sensing (DAS) as a method by which near-miss stimulated fractures may be identified and distinguished from hydraulically connected fractures. The low-frequency sub-nanostrain signatures of both complete and near-miss fractures in DAS data are simulated in this study using a hydrogeomechanical discrete fracture network model. The spatial distribution of strain was found to be an accurate indicator. However, this indicator must be evaluated in the context of DAS gauge length and spatial sampling. These simulations are a precursor to tests to be conducted at the Utah Frontier Observatory for Research in Geothermal Energy (FORGE) in 2023.

1. INTRODUCTION

An Enhanced Geothermal System (EGS) is constructed by creating flow pathways in hot, but initially impermeable, rock. The enhanced permeability allows fluid to be circulated between injection and production well pairs to extract thermal energy. Permeability is created through hydraulic fracturing or shear activation (stimulation) of the rock mass, developing a fracture network that connects wells hydraulically. The economic viability of these systems is closely tied to an even distribution of fluid flow through the fracture network. The work described here is part of a larger project (FOGMORE, Fiber Optic Geophysical Monitoring of Reservoir Evolution) aimed at characterizing and confirming efficient fluid flow in stimulated networks at the Utah Frontier Observatory for Research in Geothermal Energy (FORGE) site in Milford, Utah. The FORGE site was established by the Department of Energy (DOE) to develop EGS technologies.

To evaluate the stimulated fracture network connecting the injection well 16A(78)-32 and a planned production well 16B(78)-32, periodic hydraulic testing will be conducted. Fluid will be injected in 16A and the hydromechanical response observed in 16B. To detect the distribution of flow response in 16B, rock strain will be measured using low-frequency fiber optic distributed acoustic sensing (DAS) as well as Brillouin distributed strain sensing (DSS) observations. Fluid pressure increase in fractures will result in displacement of fractures in the connected networks, which can be measured at sub-nanostrain levels using DAS (Becker et al., 2017). Because DAS is best suited to measuring strain rate, we will enhance the dynamic fluid behavior by injecting fluid as a series of pulses. An additional objective of these experiments is to identify any stimulated fractures that are close, but do not intersect the production well, by sensing their strain shadows. These "near-miss" fractures are of interest because they may be extended to the production well by re-stimulation in targeted stages.

DAS is particularly useful for EGS monitoring due to its low cost, ability to withstand extreme subsurface conditions, positioning versatility, and long-term viability (Lellouch et al., 2020). At a sampling rate of 1kHz, a DAS interrogator measures strain rate along the fiber optic (FO) cable at paired positions separated by gauge length (Becker et al., 2017). Gauge length and channel spacing depend on the FO cable specifications. In this study, the 10 m gauge length measures strain rate at a 1 Hz sampling rate with a channel spacing of 1 m along the cable. Strain is measured only in the direction of the fiber, i.e. in-line compression and extension.

To our knowledge, hydraulic testing of this type has not been conducted at a geothermal site using DAS as the measurement modality. A numerical model of potential DAS strain was developed in COMSOL® Multiphysics. COMSOL is a generic finite element multiphysics simulator. Both complete and near-miss fractures are simulated in this study using a hydromechanical discrete fracture network (DFN) model. Expected DAS response to these simulations is achieved by post-processing the strain data in MATLAB. The modeling workflow developed in this study may be used for DAS hydraulic tests at EGS reservoirs at FORGE and elsewhere.

2. NUMERICAL MODEL

The workflow to model the FORGE reservoir and simulate DAS response to the hydraulic test is divided into five components: (1) setting up the hydromechanical model of the FORGE reservoir, (2) creating the fracture network, (3) defining FORGE granitoid parameters, (4) simulating the hydraulic test with a time-dependent study, and (5) post-processing strain data in MATLAB.

2.1 Model Set-Up

A hydromechanical model was constructed in COMSOL by coupling Solid Mechanics and Darcy's Law interfaces with the Poroelasticity multiphysics node (Figure 1). The DFN node was used to simulate the stimulated fractures. As shown in Figure 1, the model simulates injection well 16A(78)-32 and 16B(78)-32 connected by fractures within the granitoid basement at FORGE. The permeability in the DFN is many orders of magnitude larger than the rock matrix, so flow is almost entirely through fractures.

In the Solid Mechanics interface, this simplified subsurface block model is described as an isotropic linear elastic material. Elastic properties of Young's Modulus and Poisson's Ratio are specified to describe the stiffness of the porous material and deformation perpendicular to loading. In-situ stress gradients and pore pressure values derived from the Darcy-flow interface are applied to the block using the Linear Elastic Material External Stress node. The assumed maximum and minimum horizontal stress orientations are 30° and 120° respectively as described in Lee and Ghassemi (2022). Figure 1C shows that the in-situ stresses are aligned with the x- and y-axes, in which the maximum horizontal stress is applied in the y-direction. Gravity is applied to the domain. All block boundaries are free to move only in the tangential direction. The fractures are represented as thin elastic layers to model the flexibility of the fracture zone.

The Darcy's Law interface describes the block as an isotropic porous medium. The Darcian Flow model is applied, prescribing a linear pressure-velocity relationship. A poroelastic storage model is applied to the porous medium. All block boundaries are set to initial hydrostatic pressure head gradient, and gravity is applied to the domain. Two wells are included within the block, an injection well with mass flow rate specified and a production well used to measure response to injection. The production well is positioned 100 m above and parallel to the injection well; in this simulation, it serves only as a trajectory for the DAS cable i.e. flow is not permitted to the production well. Well 16A(78)-32 was drilled approximately 65° from vertical and 105° from North, so both wells are oriented in that direction and adjusted for the in-situ stress rotation (Winkler and Swearingen, 2021). For the scenario presented here, injection is specified only along a 10 cm segment at which a fracture intersects to constrain flow primarily to the single fracture intersection (see fracture network description below). The Fracture Flow node applied to all fractures defines fracture flow within the fracture geometries in the porous medium. Fracture properties include the aperture, cubic law permeability model, and material parameters.

The Poroelasticity interface couples fluid flow with solid deformation defined in the Solid Mechanics and Darcy's Law physics interfaces. This coupling allows the solid to respond to changes in flow conditions over time. The Biot's effective stress coefficient is specified to describe the distribution of external stress between pore fluid and porous matrix.

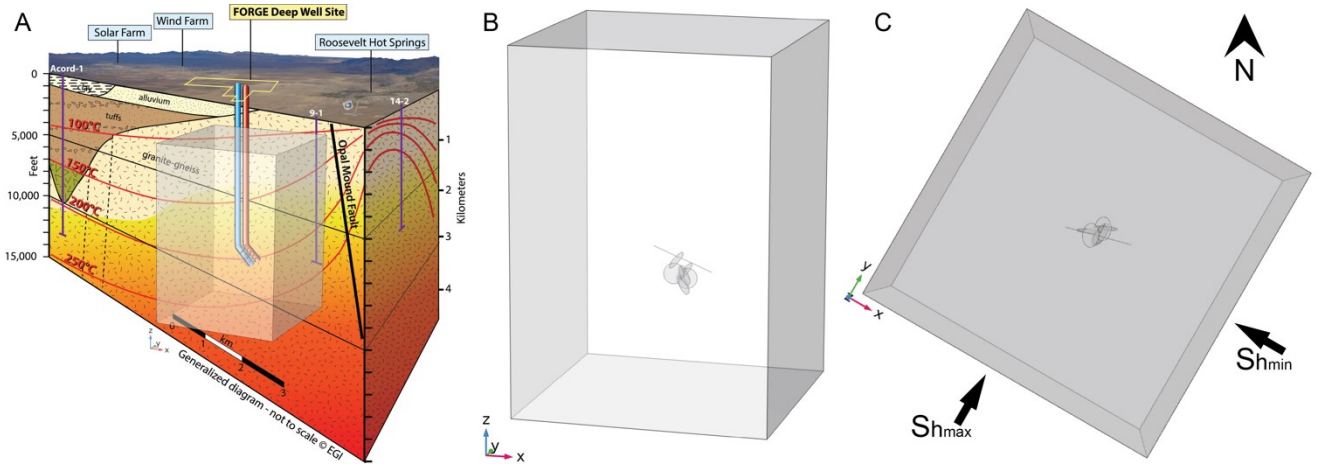

Figure 1: (A) COMSOL model simulates the granitoid basement at FORGE (Utah FORGE, 2018). (B) only a subset of the expected fractures are modeled here, and (C) the model is rotated with respect to North to align the x- and y- axes with the maximum horizontal stress (S_{hmin}) and minimum horizontal stress (S_{Hmax})

2.2 Fracture Network

The orientations of the simulated fracture network were adopted from the Utah FORGE Phase 2C Report, Section B Results II by Moore et al. (2019). Both wells in the model are connected by a six-fracture network generated by the 3D Discrete Fracture Network add-in constrained to a bounding box to represent a region of stimulated fractures, as shown in Figure 2. The DFN is simple and tightly constrained for the purposes of this study. To focus on identifying and distinguishing the strain signatures of near-miss fractures from hydraulically connected fractures, the apertures, sizes, and orientations for all 6 fractures are constant. Positions were randomly distributed, but it was required that there be at least one intersecting fracture and one near-miss fracture. The cubic-law permeability model was applied to all fractures, which have an initial aperture of 0.1 mm, and is expressed as:

$$k_f = \frac{b^2}{12} \tag{1}$$

where k_f and b represent fracture permeability and fracture aperture, respectively.

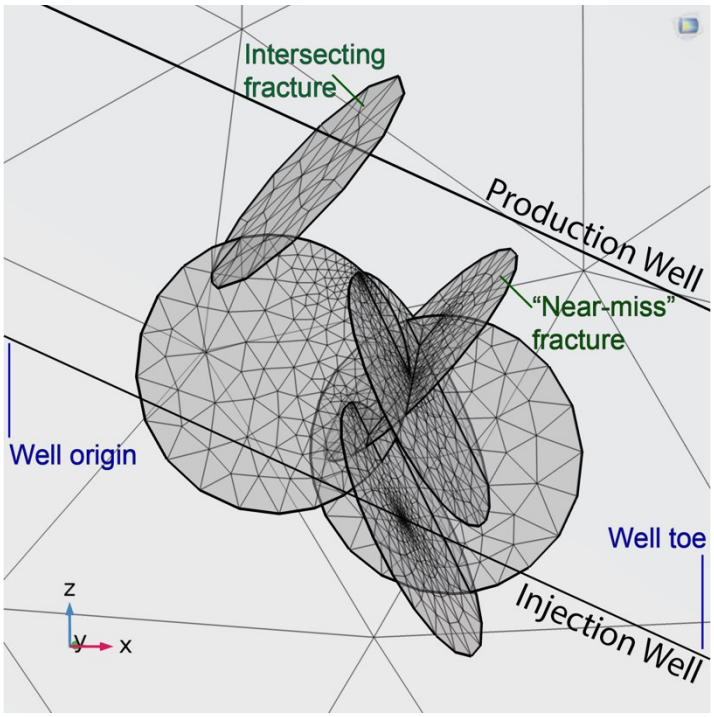

Figure 2: Fracture network connecting Injection and Production/Observation wells consists of a completely connected fracture and a "near-miss" fracture.

2.3 Input Parameters

Input parameters, derived from FORGE collaboration publications, are shown in Table 1. Fracture permeability is related to aperture as modeled by the cubic law. Water properties correspond to estimated average reservoir conditions at 200°C and 20.7 MPa described by Xing et al. (2022).

Table 1: Input parameters for FORGE EGS simulation.

Parameter	Value
Young's Modulus	54.5 GPa
Poisson's Ratio	0.29
Biot's Coefficient	0.69
Porosity	0.01
Fracture Porosity	0.5
Matrix Permeability	4.44E-17 m^2
Density of Granitoid	2670 kg/m^3
Maximum Horizontal Stress Gradient	0.0218 MPa/m
Minimum Horizontal Stress Gradient	0.0165 MPa/m
Vertical Stress Gradient	0.0256 MPa/m
Density of Water at Reservoir Conditions	878 kg/m^3
Viscosity of Water at Reservoir Conditions	1.5E-4 Pa-s
Compressibility of Water at Reservoir Conditions	8.7E-10 1/Pa

2.4 Time-Dependent Study

To simulate the hydraulic test, a time-dependent study was evaluated in COMSOL. The simulated periodic test involves a sinusoidal injection / withdrawal source term. Since DAS senses strain periodically, periodic hydraulic testing is required. Injection rates and hydraulic responses are therefore sinusoidal. The injection well is prescribed a mass flow rate of 0.1 kg/s along the injection lateral with a period of 60 minutes. Applying a sinusoidal injection mass flow rate is expressed as:

$$Q_m^* = \dot{Q}_m \times \sin\left(\frac{2\pi}{T} \times t\right) \quad (2)$$

where Q_m^*, $\dot{Q}_m$, T, and t are sinusoidal injection mass flow rate, mass flow rate, period, and time, respectively. Although a perfect sinusoid hydraulic source cannot be achieved in practice, it provides a baseline evaluation of the DAS methodology.

2.5 Post-Processing

To retrieve the axial strain along the simulated DAS fiber, the strain tensor matrix is transformed based on a rotated coordinate system aligned with the well/DAS trajectory. COMSOL output of axial strain with the corresponding arc length along the fiber is then exported for import into MATLAB. Because the fiber is initially unstrained, initial strain is removed in MATLAB to depict only the change in strain for the duration of the hydraulic test. The derivative of that strain data is calculated to give the strain rate. Both the total strain and strain rate are plotted over the duration of the test and at specific times.

Since DAS measures strain along sections of the fiber according to the gauge length instead of at individual points as COMSOL computes, the data must be processed in MATLAB. The simulated gauge length is 10 m, computed as a moving average every 1 m applied in MATLAB. This simulates the limited resolution of DAS strain rate measurements due to gauge length.

3. SIMULATION RESULTS

3.1 Simulated DAS-Measured Strain

The results of the COMSOL time-dependent study simulate strain measured along the production well over time, as shown in Figure 3. A 250 m segment of the production well is simulated, with distance along the well increasing with depth from the origin to the toe, as shown in Figure 2. In this simulation, a hydraulically connected fracture intersects the production well at 107 m distance along the well. A near-miss fracture approaches the production well around 168 m distance. The near-miss fracture is located closer to the injection point than the completely connected fracture, as shown in Figure 2. However, the connected fracture experiences larger magnitude strain as it is a constrained conduit for the strain to propagate. The strain signatures reflect the stretching and compressing/relaxing behavior of the fiber as the fluid approaches. The mechanical strain propagates in advance of the fluid pressure. Sinusoidal injection and withdrawal peak at 15 and 45 minutes, respectively. Peak strain is delayed as it takes time for the signal to propagate and reverse the flow direction.

Strain rate along the production well varies over the course of injection and withdrawal, as shown in Figure 4. Positive strain rate corresponds to extending, while negative strain rate corresponds to compressing. A change in strain rate polarity is associated with the change in direction of fluid pressure propagation. The simulated FO cable along the production well stretches as fluid pressure propagates toward the well and compresses as fluid withdraws. A stress shadow is observable around the opening of near or intersecting fractures with injection and closing with withdrawal. A dovetail pattern during fracture closing is observable, likely associated with relaxation of material that was compressed during fracture opening. This dovetail pattern is also noticeable during fracture re-opening, in which material immediately surrounding the fracture intersection is compressed to allow for extension in the fracture zone.

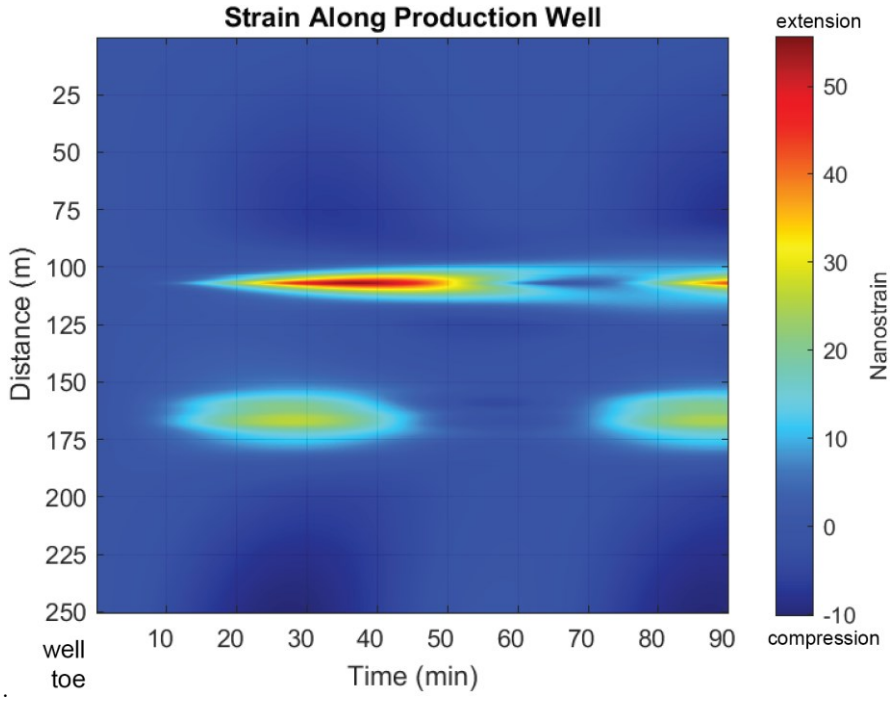

Figure 3: Nanostrain measured along the production well over time. DAS has a strain resolution of less than 1 nanostrain. The fiber is stretched as injected water travels toward the fracture and then relaxes as the fluid withdraws.

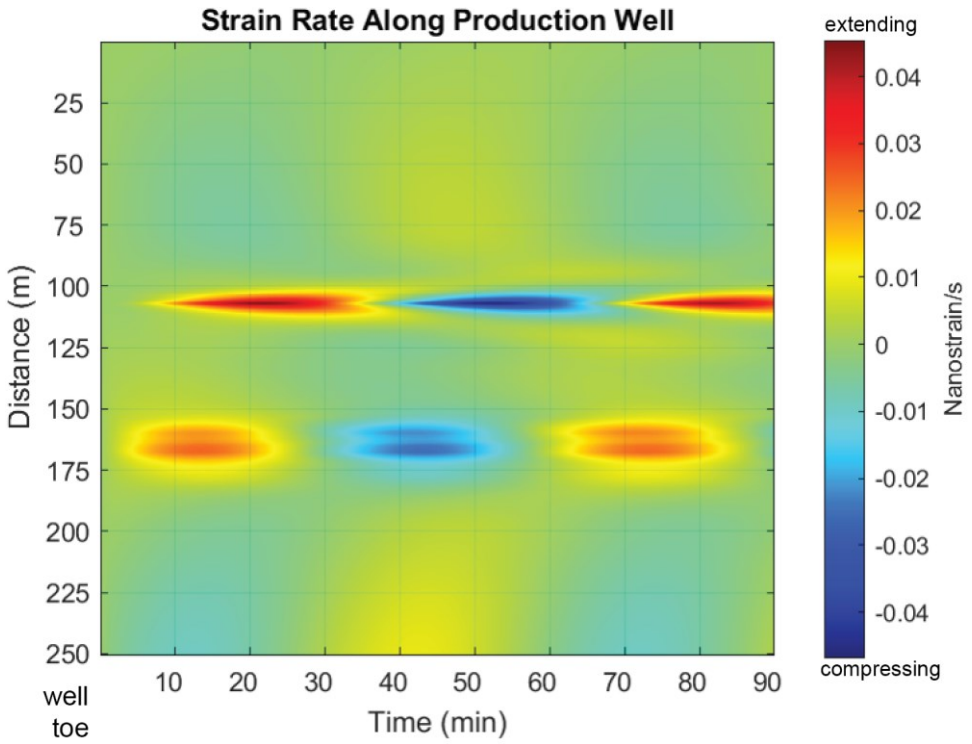

Figure 4: The strain rate along the production well over time demonstrates the change in strain rate polarity over the course of injection and withdrawal. A stress shadow is observable around the opening of the fracture with injection and closing with withdrawal. Positive strain rate values correspond to extending, and negative strain rate values correspond to compressing.

Over the course of injection and withdrawal sequence, strain rate magnitude and sign fluctuate, as shown in Figure 5. A 10 m moving average is applied in MATLAB to simulate the gauge length commonly associated with DAS. The gauge length tends to smooth the strain rate measurement in space, reducing the spatial resolution of measurement. During initial injection, both intersecting and near-miss fractures experience only tensile strain rate associated with fracture opening and fluid propagation in the direction of the production well, as shown in Figure 5(A). The "near-miss" fracture in this scenario is located closer to the injection point, allowing the strain signal to follow the injection and withdrawal rate more closely. The connected fracture in this scenario therefore has a delayed signal compared to the "near-miss," as shown in Figure 5(B). Figure 5(C) shows that the strain shadow associated with the closing intersecting fracture and the relaxation of surrounding material is observable even with gauge length applied. After the withdrawal signal has had time to propagate before injection resumes, both fractures experience compressive strain, as shown in Figure 5(D).

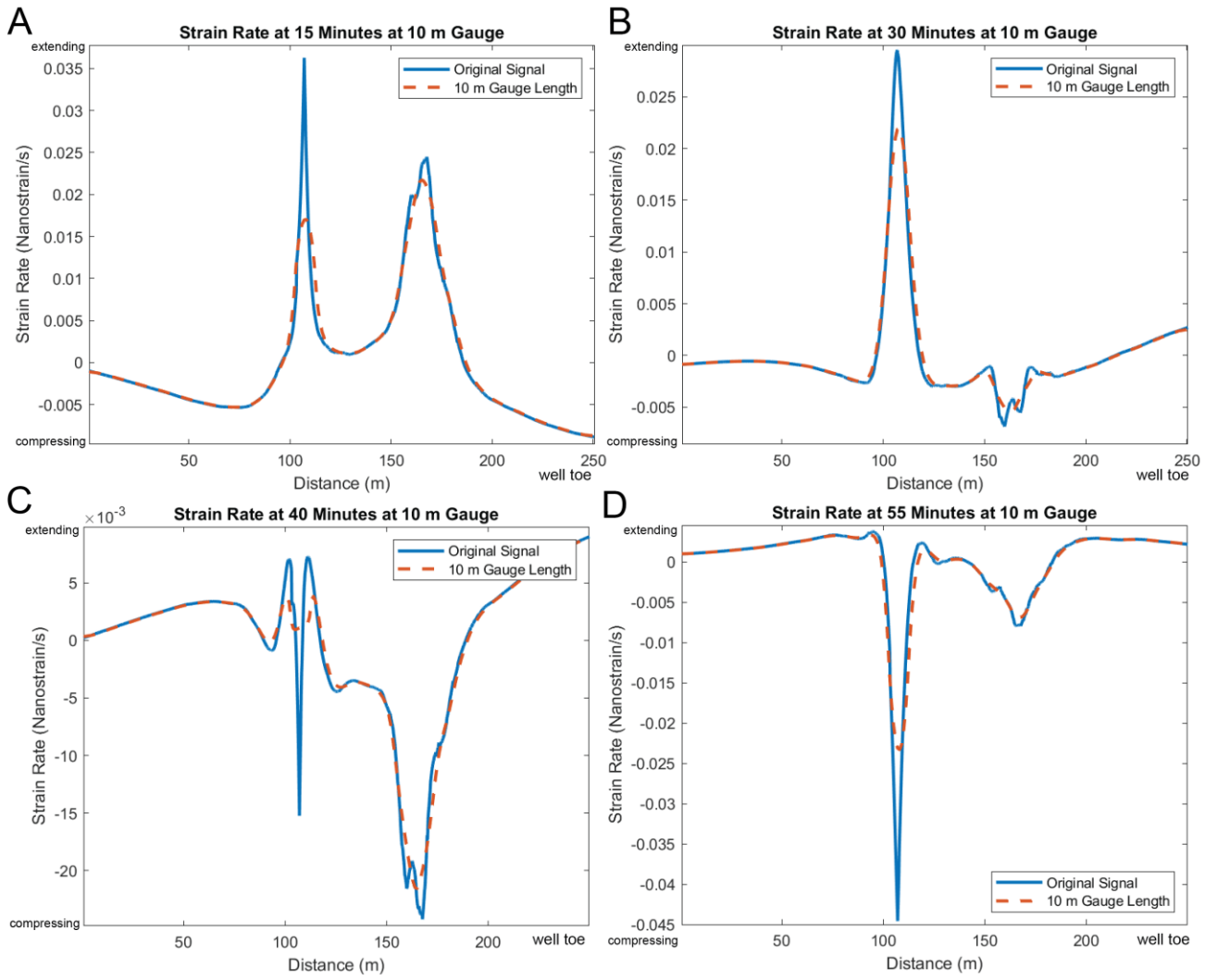

Figure 5: Strain rate along the distance of the well varies over the course of injection and withdrawal. DAS strain rate measurements limited by gauge length are estimated by applying a 10 m moving average window. Positive strain rate values correspond to extending, and negative strain rate values correspond to compressing.

3.2 Variations Due to Fracture Geometry

To demonstrate that near-miss fractures can be identified under different circumstances, DFN geometry variations are simulated, as shown in Figure 6. The injection rate and period are the same as the previous simulation, with a mass flow rate of 0.1 kg/s and a 60-minute period. The strain rate signature in the DAS data are a function of the distance and orientation of the fracture with respect to the DAS fiber. Figure 6(A) shows a model with one intersecting fracture and two near-miss fractures. The fracture located around 160 m is closer and more hydraulicly connected to the injection well compared to the fracture at around 74 m. The more hydraulically connected near-miss fracture is associated with a larger magnitude signal than the other near-miss. The near-miss fracture located further from the injection well approaches closer to the production well than the other near-miss, but it approaches at an angle, thus distributing the fluid pressure and strain signal over a wider area along the well. Figure 6(B) shows a model with the intersecting fracture located closer to the injection source and the near-miss fracture located further compared to the first model shown in Figure 2. Both signals are discernable. Figure 6(C) shows a model with both the near-miss and intersecting fractures located close to each other and further from the injection source. The proximity between the two fractures makes it more difficult, but still possible, to discern both positions.

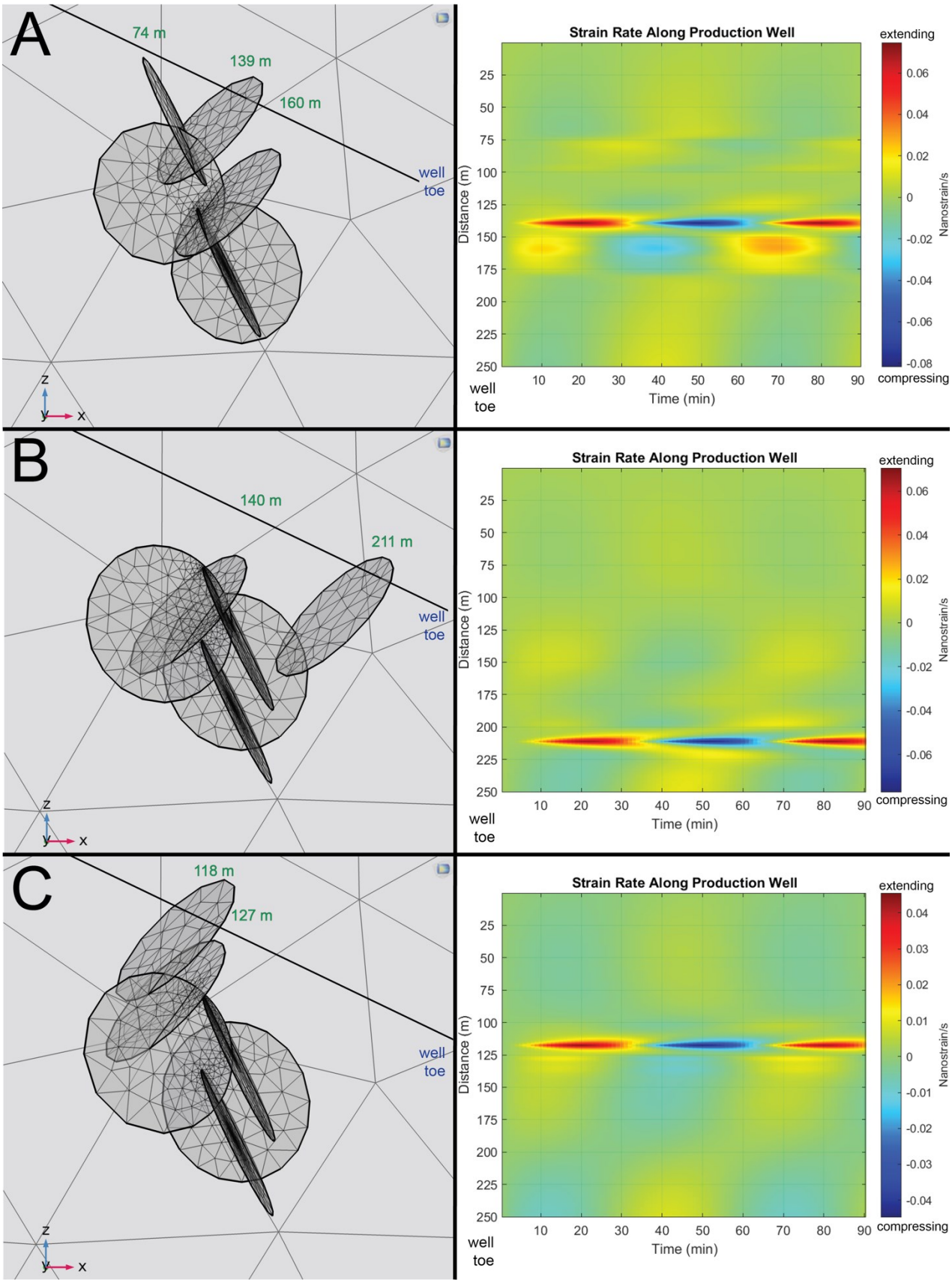

Figure 6: Fracture orientations are adjusted to simulate strain rate along the well over time associated with geometry variations. The distance along the production well at which either a fracture intersects or a "near-miss" approaches is labeled.

3.3 Distinguishing Near-Miss Fractures from Intersecting Fractures

Hydraulically connected, well-intersecting fractures are characterized by large magnitude, sharp strain rate signals, whereas "near-miss" fractures are characterized by smaller magnitude, broad signals. Both near-miss and intersecting fractures correspond to stress shadows surrounding the fracture location. Dovetail signatures (e.g. Figure 6) characterize the regions just outside the fracture zone to make room for the relaxing of local material. These dovetail signatures may be less obscured by DAS gauge length limitations for intersecting fractures. Near-miss fractures are associated with less extreme dovetail signatures as there is no opening or closing of a fracture or fluid propagation directly along the well. Near-miss fractures that are oriented obliquely to the direction of the DAS fiber will produce a broader and lower magnitude strain rate response than those oriented perpendicular to the DAS fiber.

4. CONCLUSIONS

A hydromechanical model simulates the low-frequency sub-nanostrain signatures of both complete and near-miss fractures observable by DAS. These simulations are a precursor to hydraulic tests to be conducted at the Utah Frontier Observatory for Research in Geothermal Energy (FORGE) to evaluate the stimulated fracture network between the injection and production well. The model constructed with COMSOL Multiphysics software simulates the FORGE reservoir and DAS hydromechanical response to the hydraulic test. Our simulations indicate that near-miss hydraulically connected fractures may be identified and distinguished from intersecting hydraulically connected fractures through DAS data analysis. By locating near-miss fractures, it may be possible to re-stimulate and extend these fractures and thus improve hydraulic connectivity between injector-producer well pairs.

AKNOWLEDGEMENTS

Funding provided by DOE EERE Geothermal Technologies Office to Utah FORGE and the University of Utah under Project DE-EE0007080 Enhanced Geothermal System Concept Testing and Development at the Milford City, Utah Frontier Observatory for Research in Geothermal Energy (Utah FORGE) site. The authors would like to thank the FOGMORE team for their valuable teamwork and discussion.

REFERENCES

Becker, M.W., Ciervo, C. and Coleman, T., 2018, February. A slimhole approach to measuring distributed hydromechanical strain in fractured geothermal reservoirs. In Proceedings of the 43rd Workshop on Geothermal Reservoir Engineering Stanford University, Palo Alto, CA, USA (pp. 12-14).

Becker, M.W., Ciervo, C., Cole, M., Coleman, T. and Mondanos, M., 2017. Fracture hydromechanical response measured by fiber optic distributed acoustic sensing at milliHertz frequencies. Geophysical Research Letters, 44(14), pp.7295-7302.

Becker, M.W., Coleman, T.I. and Ciervo, C.C., 2020. Distributed acoustic sensing as a distributed hydraulic sensor in fractured bedrock. Water Resources Research, 56(9), p.e2020WR028140.

Finnila, A., Forbes, B. and Podgorney, R., 2019, February. Building and utilizing a discrete fracture network model of the forge Utah site. In Proceedings of the 44th Workshop on Geothermal Reservoir Engineering, Stanford University, Stanford, CA, USA (pp. 11-13).

Guiltinan, E. and Becker, M.W., 2015. Measuring well hydraulic connectivity in fractured bedrock using periodic slug tests. Journal of Hydrology, 521, pp.100-107.

Jin, G. and Roy, B., 2017. Hydraulic-fracture geometry characterization using low-frequency DAS signal. The Leading Edge, 36(12), pp.975-980.

Jin, G., Ugueto, G., Wojtaszek, M., Guzik, A., Jurick, D. and Kishida, K., 2021. Novel Near-Wellbore Fracture Diagnosis for Unconventional Wells Using High-Resolution Distributed Strain Sensing during Production. SPE Journal, 26(05), pp.3255-3264.

Lee, S.H. and Ghassemi, A., 2022. Numerical simulation of fluid circulation in hydraulically fractured Utah FORGE wells. In Proceedings of the 47th Workshop on Geothermal Reservoir Engineering.

Lellouch, A., Lindsey, N.J., Ellsworth, W.L. and Biondi, B.L., 2020. Comparison between distributed acoustic sensing and geophones: Downhole microseismic monitoring of the FORGE geothermal experiment. Seismological Society of America, 91(6), pp.3256-3268.

Moore, J., Simmons, S., McLennan, J., Jones, C., Skowron, G., Wannamaker, P., Nash, G., Hardwick, C., Hurlbut, W., Allis, R. and Kirby, S., 2019. Utah FORGE: Phase 2C topical report (No. 1187). USDOE Geothermal Data Repository (United States); Energy and Geoscience Institute at the University of Utah.

Ugueto, G.A., Wojtaszek, M., Mondal, S., Guzik, A., Jurick, D. and Jin, G., 2021, July. New Fracture Diagnostic Tool for Unconventionals: High-Resolution Distributed Strain Sensing via Rayleigh Frequency Shift during Production in Hydraulic Fracture Test 2. In SPE/AAPG/SEG Unconventional Resources Technology Conference. OnePetro.

Winkler, D. and Swearingen, L., 2021. Summary of Drilling Activities: Well 16A (78)-32.

Xing, P., Damjanac, B., Moore, J. and McLennan, J., 2022. Flowback Test Analyses at the Utah Frontier Observatory for Research in Geothermal Energy (FORGE) Site. Rock Mechanics and Rock Engineering, 55(5), pp.3023-3040.

Xing, P., McLennan, J. and Moore, J., 2020. In-Situ Stress Measurements at the Utah Frontier Observatory for Research in Geothermal Energy (FORGE) Site. Energies, 13(21), p.5842.

Xing, P., Wray, A., Arteaga, E.I.V., Finnila, A., Moore, J., Jones, C., Borchardt, E. and McLennan, J., 2022. In-situ stresses and fractures inferred from image logs at Utah FORGE.

Xing, P., Damjanac, B., Radakovic-Guzina, Z., Finnila, A., Podgorney, R., Moore, J. and McLennan, J., 2021. Numerical Simulation of Injection Tests at Utah FORGE Site. In Proceedings of the 46th Workshop on Geothermal Reservoir Engineering, Stanford University, Stanford, CA, USA, February 16 (Vol. 18).

Zhang, Z., Fang, Z., Stefani, J., DiSiena, J., Bevc, D., Lim Chen Ning, I., Hughes, K. and Tan, Y., 2020. Modeling of fiber-optic strain responses to hydraulic fracturing. Geophysics, 85(6), pp.A45-A50.